Programmable fluorogenic enzyme-responsive micellar nanoparticles

M.-P. Chien*, M.P. Thompson**, and N.C. Gianneschi***

*University of California, San Diego, CA, USA, m1chien@ucsd.edu
** University of California, San Diego, CA, USA, matthewpthompson@gmail.com
*** University of California, San Diego, CA, USA, ngianneschi@ucsd.edu

ABSTRACT

We developed enzyme-responsive fluorogenic micellar nanoparticles with detectable spectrophotometric properties unique to the particles and their aggregated state. These micelles are assembled from peptide–polymer amphiphiles (PPAs) labeled with either fluorescein or rhodamine. This is achieved by labeling otherwise similar block copolymer amphiphiles with each of the dyes. When mixed together, signals from the FRET-pair can be utilized to detect particle assembly and hence enzymatic activity. Furthermore, we show FRET signals within the shell of the assembled micelles can be used to estimate particle stability (critical aggregation concentration). This system is designed to be applied in physiologically relavant settings, having broad implications for the design of nanoscale materials in drug delivery and diagnostics.

Keywords: nanoparticles, FRET, drug delivery

1 INTRODUCTION

Enzymes are unique as biomarkers because they amplify detection events by catalytic turnover with selectivity that can be specific to given disease states [1–4]. The specificity and diversity of reactions catalyzed by enzymes and their importance as signalamplifying biomarkers make them exceptionally attractive as tools in the assembly and manipulation of nanoscale materials [5]. In particular, nanoparticles capable of undergoing enzyme programmed assembly, or morphology switches are of interest because unlike substrates such as fluorogenic oligopeptides, they can theoretically act as carriers of payloads that include specific molecular diagnostics and drugs. Although underutilized, enzymes have been harnessed as selective tools for the manipulation of nanoscale structures, a process that in itself constitutes a unique signaling event indicating enzyme activity [5–9]. Such responses have proven detectable based on routine morphology analyses via methods including electron microscopy and light scattering. However, changes in nanoscale architecture will only be detectable in more challenging settings (e.g. *in vivo*) if the action of the enzyme results in an output signal unique to the assembly, such as a spectrophotometric response. To enable this, we have developed peptide–polymer amphiphiles (PPAs) [10,11] linked to dyes [12] capable of undergoing efficient Forster Resonance Energy Transfer (FRET) for detecting structural properties and aggregation states of self-assembled enzymeresponsive nanoparticles. Herein, this concept is demonstrated for elucidation of particle stability, particle structure, and for monitoring enzyme-induced morphological transformations (Fig. 1).

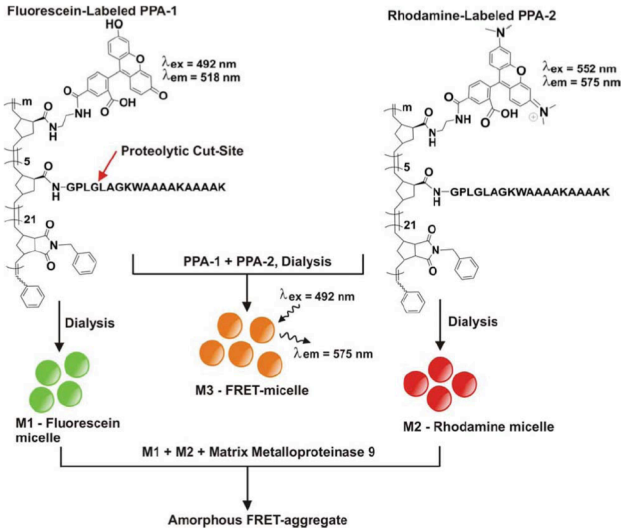

Figure 1. Assembly of peptide–polymer amphiphiles (PPAs) to generate fluorogenic micellar nanoparticles. Adapted from *Chem. Sci.* 2012.

2 RESULTS AND DISCUSSION

The PPAs utilized in these studies were designed as substrates for the cancer-associated enzyme, matrix-metalloproteinase 9 (MMP-9). By utilizing this substrate as the polar head group of the copolymer, the micelle morphology and aggregation behaviour of the materials could be modified via peptide cleavage by MMP at the Gly–Leu peptide bond (Fig. 1). We reasoned that enzymatic reactions occurring within the shell of the particles would facilitate a dramatic reduction in the hydrophilicity of the peptide-block, and would subsequently result in changes to the overall architecture via the establishment of new equilibria for surfactant aggregation. The polymers were synthesized using ring-opening metathesis polymerization to generate block copolymers of a phenyl-modified

norbornene as the hydrophobic block, a conjugatable NHS-ester for linkage through the amine terminus of the peptide, and a short block of primary amino modified norbornene, for conjugation to dyes. As shown in Fig. 1, micelles of fluorescein labelled PPA-1 (M1) and rhodamine labelled PPA-2 (M2) were prepared by dialysis of solutions of the polymers in DMSO/DMF (1 : 1) against buffered water over 24 h. In addition, micelles were prepared from mixtures of the two PPAs to generate the FRET-micelle, M3.

We aimed to develop a method that allows an accurate determination of the arrangement of polymeric amphiphiles packed within micelles and to monitor structural changes induced by responses to enzymes. Moreover, this method should be amenable to use in complex environments where other particulates may be present. Such solutions containing mixtures of particles are not easily amenable to analysis by light scattering or TEM image analysis. We determined that the distance dependence of FRET efficiency of appropriately paired dyes would provide such a route and indeed, has been extensively utilized in biochemical systems. However, the use of FRET efficiency for elucidating structural parameters in supramolecular self-assembled systems has been surprisingly limited, despite its great potential in determining solution phase structures of multicomponent assemblies. Relevant and notable exceptions involve the use of fluorescence energy transfer for studying interfacial regions in the assembly of nanoparticles and micelles. Here, we demonstrate that in addition to enabling a direct measurement of exceptionally low CAC for micelles, and FRET labeled PPAs can be utilized to sensitively monitor micellar nanoparticle response to enzymes.

2.1 Characterization of Fluorogenic Enzyme-responsive Micellar Nanoparticles

Initially, the fluorescence spectra and efficiency of FRET for a range of concentrations of PPA-1 and PPA-2 in the formation of micelles was studied (Fig. 2). M1, M2 and M3, are 35–40 nm in diameter as characterized by TEM (Fig. 2a for M3) and by DLS (Fig. 2b). The two single dye labeled micelles have the expected spectroscopic properties, with a peak due to fluorescein at 512 nm for M1 and no observable fluorescence upon excitation at 470 nm for M2 (Fig. 2c). However, blending PPA-1 and PPA-2 to form M3 provides a mixed dye micelle with fluorescent properties indicative of a FRET pair within the Forster radius as evidenced by rhodamine fluorescence observable at 563 nm. At PPA concentrations above 1 mM we found that the ratio of the intensities of each peak maximum (**I**563/**I**512) is constant. This indicates the maximum FRET efficiency possible for this system (Fig. 2d). However, upon dilution of M3 over the range from 2.5 mM to 2 nM, a greater decrease in intensity of the peak at 563 nm (rhodamine) compared to 512 nm (fluorescein) is observed. Therefore, a CAC of 8 nM is assigned for M3 as the concentration at which the onset of a detectable FRET signal is observed. This is a generalizable approach providing, in this case, an exceptionally sensitive and direct method for determining CAC. Such a labeling strategy for observing intact particles is especially useful in cases where they are particularly stable, limiting the utility of standard CAC determination assays using non-covalently associated solvochromatic dyes where the limit of detection is significantly above CAC. Indeed, we have had no success implementing standard assays with regards to these systems and gathering accurate data at low concentrations. Direct labeling of the polymers also means they can be observed in complex milieu without the need for additional dye additives as will be highlighted in the context of enzymatic studies (*vide infra*).

2.2 Enzymatic Reaction of Fluoregenic Nanoparticles

PPA-1 and PPA-2 were designed as substrates for MMPs. Therefore, we sought to study enzyme-induced rearrangement of the micelles, aiming to analyze the process via fluorescence spectroscopy in buffer solutions (Fig. 3). Furthermore, to demonstrate the utility of FRET in analyzing micelle behavior in biological milieu, we examined their response to MMP-9 in blood serum doped samples of cell-growth media. Initial experiments were conducted to study enzyme kinetics on the micelle based substrates. These were conducted by preparing a micelle

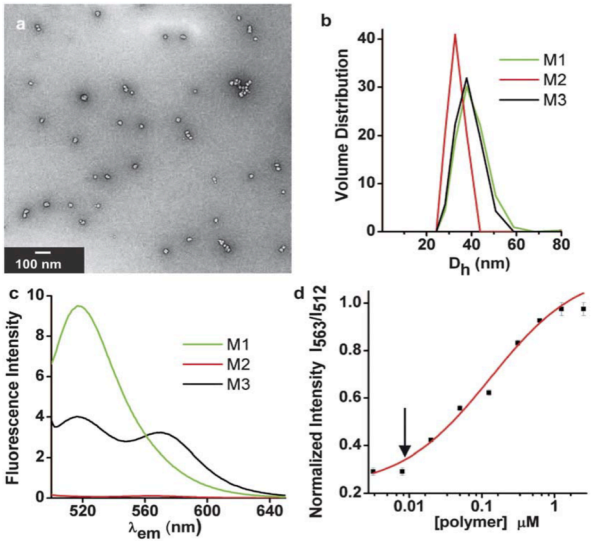

Figure 2. TEM, DLS and fluorescence spectroscopy of fluorogenic micelles. a) TEM of 30 nm M3. b) DLS of M1, M2 and M3 showing hydrodynamic diameters (**D**h) in the range of 30–40 nm. c) Fluorescence emission spectra of M1, M2 and FRET-micelle, M3 upon excitation at 470 nm. d) Ratio of normalized emission intensity for maxima at 563 nm (rhodamine) and 512 nm (fluorescein) over a range of concentrations of PPA-1 and PPA-2 upon excitation at 470 nm. Arrow indicates onset of detectable FRET. Adapted from *Chem. Sci.* 2012.

Micelle[a]	MMP-9	Solution conditions[b]	Fluorescence lifetime, t (ns)
M1	–	20% serum	3.94 ± 0.03
M1	+	20% serum	3.93 ± 0.01
M1 + M2	–	20% serum	3.93 ± 0.01
M1 + M2	+	20% serum	0.56 ± 0.02
M1 + M2	+	no serum	0.59 ± 0.01

Table 1. Detection of MMP-9 at 10 nM in blood serum doped DMEM, cell growth medium. Adapted from *Chem. Sci.* 2012.

from a PPA, end-labeled with fluorescein and conjugated to a peptide labeled with Dabcyl as a quencher, that when cleaved resulted in an ON-switch of fluorescence. These studies confirm that kinetics were similar on both particle-linked substrates and simple oligopeptide substrates. Next, we mixed M1 and M2 together with purified, commercial MMP-9 and observed the emission spectra over time (Fig. 3a) showing the formation of a new FRET-active species in solution as PPAs are cleaved and rearrange into aggregates containing both dyes. We note that peptide cleavage rates and formation of the new FRET signal, indicating aggregate formation, are similar and therefore consistent with them being concomitant processes. The peptide fragments could be quantified by HPLC (41% cleavage efficiency after 24 h), and characterized by MALDI. This low efficiency may be due to steric hinderance within the particle shells, or within the aggregates as they form during the reaction. Despite this, the particles are sufficiently susceptible to allow a complete shift to the aggregated species as evidenced by DLS. Furthermore, the FRET efficiency calculated from donor lifetimes is comparable to, but is reduced for these aggregates (efficiency 85%) compared to M3 (efficiency 93%). In addition, the relative inhomegeneity of the aggregates compared to the control particles (M3) is observed by comparison of ratios of donor and acceptor intensities in Fig. 2c (1 : 0.8) vs. Fig. 3a (1 : 0.43). This is consistent with a less homogeneous distribution of donors and acceptors. Despite this slight decrease in FRET efficiency, the response is clearly observable down to 10 pM of MMP-9 for solutions containing 0.5 mM of micelles (Fig. 3b – concentration of micelles is with respect to PPA in each case). Furthermore, MMP-9 at 10 nM is observable down to 20 nM of PPA (Fig. 3c), a result that is consistent with the exceptional stability of these aggregates with CACs in the range of 10 nM. In addition, M1 and M2 underwent enzyme-induced aggregation when treated with a mixture of expressed MMPs (Fig. 3d). We note that these particles were designed to be responsive to both cancer-associated enzymes MMP-2 and MMP-9 as expected for the substrate sequence chosen. These experiments were performed by treating M1 and M2 with cell growth media containing MMPs excreted over 24 h from WPE1-NA45 cells, and present at 0.048 nM and 0.005 nM (MMP-2 and -9 respectively) as determined by a quantitative ELISA assay. In this case, substrate concentrations of 100 nM (with respect to PPAs) resulted in observable responses within 4 h reaction time. Finally, this enzyme-induced rearrangement of PPAs was characterized by TEM, confirming the formation of a new aggregated species upon cleavage of the peptide sequence in M1 and M2 (Fig. 3e–f). It is this aggregated species that carries both dyes, in close enough proximity to allow spectroscopic characterization by FRET. To demonstrate the utility of the

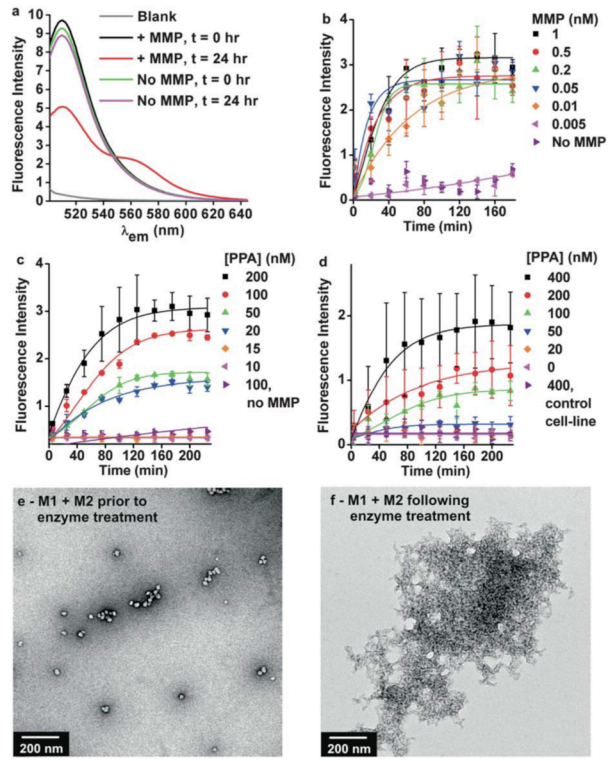

Figure 3. Response of mixtures of M1 and M2 to MMPs. a) Fluorescence spectra of M1 and M2 (0.5 mM each with respect to PPA) with and without MMP-9 (10 nM) at times indicated following enzyme addition; λ_{ex}: 470 nm. b–d) Fluorescence intensity vs. time plots via plate reader analysis, to monitor rearrangement of PPA-1 and PPA-2 into new FRET active aggregates; λ_{ex}: 490 nm and λ_{em}: 590 nm. b) Detection of MMP-9 down to 10 pM of enzyme with M1 and M2 (at 0.5 mM, [PPA]). c) Detection of MMP-9 at 10 nM with varying concentrations of M1 and M2 shown with respect to [PPA], detectable down to 20 nM of polymer. d) Detection of cell-secreted (WPE1-NA45 cells) MMP-2 and -9 with varying concentrations of M1 and M2 shown with respect to [PPA]. Cells were seeded at 1.6×10^4 cells/well in a clear bottom 96-well plate in DMEM. After 24 h, cell medium was added to solutions of M1 and M2. MMP-2 and -9 were at 0.048 nM and 0.005 nM respectively as quantified by an ELISA. Control was the non-MMP expressing MCF-7 cell-line cultured in the same manner. All reactions run in PBS, unless otherwise noted. e–f) TEM of M1 and M2 before and after 24 h following MMP-9 treatment. Adapted from *Chem. Sci.* 2012.

labeling approach in the detection of enzymes in more complex media, we mixed M1 and M2 in blood serum doped cell media samples and treated them with MMP-9 (Table 1). This resulted in an easily detectable and significant shortening of the fluorescence lifetime.

3 CONCLUSIONS

We have described nanoparticles that undergo enzyme-induced changes in structure which are detectable in complex environments. This is a necessary step in the future implementation of enzyme-programmed materials in *in vivo* applications. In particular, where enzymatic signals are specific to given disease states including inflammation and metastasis. This is enabled by a labeling approach that provides critical information regarding particle structure and stability. Together, these studies are consistent with exceptionally stable micelles that show no detectable scrambling of PPAs when mixed together in the absence of MMP. Moreover, the enzymatic response constitutes a novel approach to the detection of enzymes whereby the stimulus induces detectable changes in nanoparticle morphology. We note that this is not intended as a technology towards sensitive diagnostic detection of enzymes *in vitro*, but rather for analyzing and utilizing the response of nanomaterials to enzymes as they undergo complex changes in structure. We are examining this labeling approach for its utility in monitoring the response of nanoparticles to disease-associated enzyme activity *in vivo*. Figure 4 shows the *in vitro* fluorescence imaging of M1/M2, M1, M3, and $M1_D/M2_D$ (control nanoparticles with *D*-amino acid based substrates, which can not be cleaved by MMPs) with or without addition of MMPs. These samples were excited at 470 nm and monitored at 590 nm as an indicator of the developing FRET signal (quenched, redish color in Fig. 4). The FRET signal can be clearly seen in M3 (FRET positive nanoparticles) and M1/M2+MMP (aggregation driven FRET signal). Animal studies are currently underway in our laboratories via the fluorescence imaging method shown in Fig. 4. This system will have implications for the design of nanoscale materials in drug delivery and diagnostics.

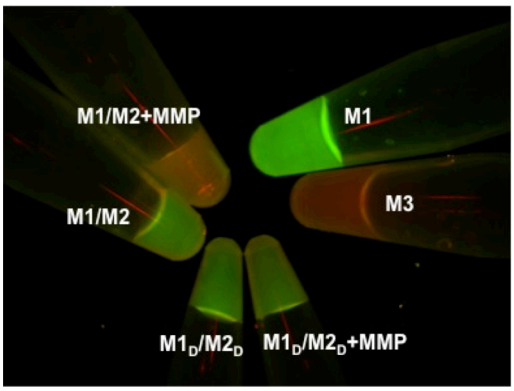

Figure 4. Fluorescence imaging of fluorogenic nanoparticles. Different mixture of fluorogenic nanoparticles are treated with or without MMP enzymes as shown in the figure. Note: $M1_D$ or $M2_D$ are the control nanoparticles same as M1 and M2 except the peptide substrates are *D*-amino aicds. λ_{ex}: 490 nm and λ_{em}: 590 nm.

REFERENCES

[1] R. K. Saiki, S. Scharf, F. Faloona, K. B. Mullis, G. T. Horn, H. A. Erlich and N. Arnheim, Science, 230, 1350–1354, 1985.
[2] E. Engvall and P. Perlmann, Immunochemistry, 8, 871–874, 1971.
[3] L. Zhu and E. V. Anslyn, Angew. Chem., Int. Ed., 45, 1190–1196, 2006.
[4] T. Jiang, E. S. Olson, Q. T. Nguyen, M. Roy, P. A. Jennings and R. Y. Tsien, Proc. Natl. Acad. Sci. U. S. A., 101, 17867–17872, 2004.
[5] M. E. Hahn and N. C. Gianneschi, Chem. Commun., 47, 11814, 2011.
[6] G. Von Maltzahn, T. J. Harris, J.-H. Park, D.-H. Min, A. J. Schmidt, M. J. Sailor and S. N. Bhatia, J. Am. Chem. Soc., 129, 6064–6065, 2007.
[7] T. H. Ku, M. P. Chien, M. P. Thompson, R. S. Sinkovits, N. H. Olson, T. S. Baker and N. C. Gianneschi, J. Am. Chem. Soc., 133, 8392–8395, 2011.
[8] R. J. Amir, S. Zhong, D. J. Pochan and C. J. Hawker, J. Am. Chem. Soc., 131, 13949–13951, 2009.
[9] R. V. Ulijn, J. Mater. Chem., 16, 2217–2225, 2006.
[10] H. Cui, M. J. Webber and S. I. Stupp, Peptide Sci., 94, 1, 2010.
[11] C.-L. Chen, P. Zhang and N. L. Rosi, J. Am. Chem. Soc., 130, 13555–13557, 2008.
[12] H. A. Behanna, K. Rajangam and S. I. Stupp, J. Am. Chem. Soc., 129, 321–327, 2007.